LAWRENCE
LIVERMORE
NATIONAL
LABORATORY

LLNL-JRNL-635613

Temperature dependent 780-nm laser absorption by engineering grade aluminum, titanium, and steel alloy surfaces

A. M. Rubenchik, S. S. Wu, V. K. Kanz, W. H. Lowdermilk, M. D. Rotter, J. Stanley

April 22, 2013

Optical Engineering

Disclaimer

Temperature dependent 780-nm laser absorption by engineering grade aluminum, titanium, and steel alloy surfaces

A.M. Rubenchik, S.S.Q. Wu, V.K. Kanz, W.H. Lowdermilk, M.D. Rotter, J.R. Stanley

Lawrence Livermore National Laboratory, Livermore, CA 94550

Abstract

Modeling of laser interaction with metals for various applications requires knowledge of absorption coefficients for real, commercially available materials with engineering-grade (unpolished, oxidized) surfaces. However, most absorptivity data currently available pertain to pure metals with polished surfaces or vacuum-deposited thin films in controlled atmospheres. One reason for lack of data on real materials is that measurements are complicated by the dependence of absorptivity on numerous material and laser parameters as well as on sample temperature. This paper presents results of absorptivity measurements as a function of temperature on as-received, engineering grade aerospace alloys: aluminum, titanium, and steel. Direct calorimetric measurements were made using a diode-array laser emitting at 780 nm. The absorptivity results obtained differ considerably from existing data for polished pure metals, and are essential to development of predictive laser-material interaction models.

Introduction

Measurement of absorptivity is important for analysis and modeling of laser-material interactions. Absorption of laser light depends on laser parameters: intensity, wavelength, polarization and angle of incidence, and material properties including composition, temperature, surface roughness, oxide layers and contamination. Theoretical and experimental studies of absorptivity and reflectance of metals have concentrated on perfectly pure, clean and flat surfaces, free of oxide layers, unlike real life material processing applications where metal surfaces are rough to some extent, and contaminated with impurities and oxide layers. Also,

little information is available on absorptivity of alloys, which in real processing applications are far more commonly used than pure metals. Thus published values of absorptivity for pure polished surfaces are inadequate for laser-material interaction models. In addition, detailed analysis and modeling of laser material interactions require material absorptivity over a wide range of temperature. The standard collection of textbooks [1] has data mainly for ideal materials at room temperature. In engineering applications, metals are oxidized and have impurities, surface irregularities and defects; hence their absorptivity can be considerably different from handbooks values [2].

Lasers have been widely used for many years for various material processing applications. In situations that do not require narrow linewidth laser beams, where the laser acts as an energy source only, the more energy-efficient diode-array lasers can be used. Such lasers are now commercially available in a wide variety of wavelengths and formats, and were used as radiation sources in these experiments.

Direct absorptivity measurements are difficult due to the need to change the sample temperature in controlled way. Absorptivity is usually determined indirectly as the residual of measured reflectivity [3]. However, reflectance is difficult to measure accurately due to diffuse scattering and thermal radiation, especially for measurements at high temperature. To avoid these problems, direct calorimetry was used here in which a thin sample is heated uniformly by a diode array and the temperature evolution measured using thermocouples and (or) an infrared camera. The small thickness provides temperature uniformity across the sample. Heat losses due to the convection and thermal radiation are derived directly from experimental data, and by subtracting it, the temperature dependent absorptivity at wavelength of 780 nm is obtained.

This study focuses on absorptivity of aluminum, with some data for titanium and steel also presented. Extensive previous theoretical and experimental work on aluminum allows comparison of absorptivity for the engineering grade samples and ideal metals, and the various mechanisms that increase absorptivity in real

materials are discussed. In addition, the measurement of thermal loss as a function of temperature contains information about both convective loss and thermal radiative loss, which is also discussed.

Experimental set-up and measurement procedure

For direct, calorimetric absorptivity measurements, a thin sample is heated by the diode laser array and temperature evolution is measured using thermocouples, as illustrated schematically in Figure 1. The sample is thermally isolated, and all heating is produced by the absorption of laser light. The irradiation is approximately uniform over the sample. At some moment, the radiation is turned off, and the sample cools via thermal radiation and convection cooling. For the thin samples used, the thermal diffusion time is much shorter than the heating time, so temperature is expected to be uniform throughout the sample.

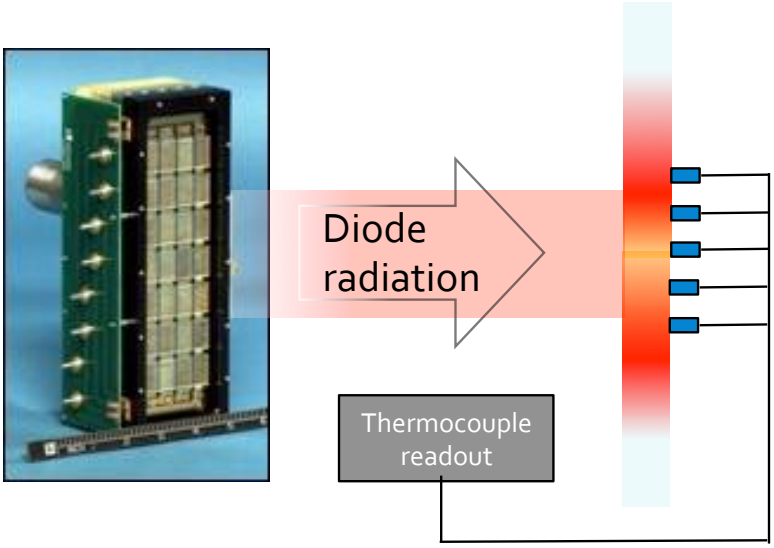

Figure 1. Experimental arrangement. Light from a diode laser array is transported optically (not shown) to a metal sample with attached thermocouples.

For a sample with uniform temperature distribution (uniform irradiation and thin sample), the temperature dependent absorptivity $A(T)$ is determined by the relation

$$w\rho(T)c_P(T)\frac{\partial T}{\partial t} = A(T)I - Q(T) \quad (1)$$

where w is the sample thickness, $\rho(T)$ the density, c_p the temperature dependent specific heat, I the incident intensity, and $Q(T)$ the thermal loss. Assuming thermal loss is a function only of sample temperature, *i.e.* the loss channels are identical with and without laser illumination, $Q(T)$ measured during cooling when the laser is off applies also during heating, then absorptivity of the sample can be determined with no ambiguity.

Square samples of industrial grade aluminum, 1-mm thick and 3x3 cm wide, were used in these measurements. The diode-array laser produced up to 3-kW power at 780 nm. Radiation was transported to the target through a fused silica "duct" that spatially smoothed the intensity distribution, as shown in Figure 2, by multiple reflections from the walls to a uniformity of +/- 5%. Intensity at the sample was limited to 10-40 W/cm^2 to heat the target slowly enough for convective cooling to be in a steady state regime and to improve temporal resolution of temperature recording. Sample temperature was measured by up to five thermocouples distributed over the surface to verify uniformity of the temperature, as shown in Figure 3 where typical data from five different thermocouples are presented.

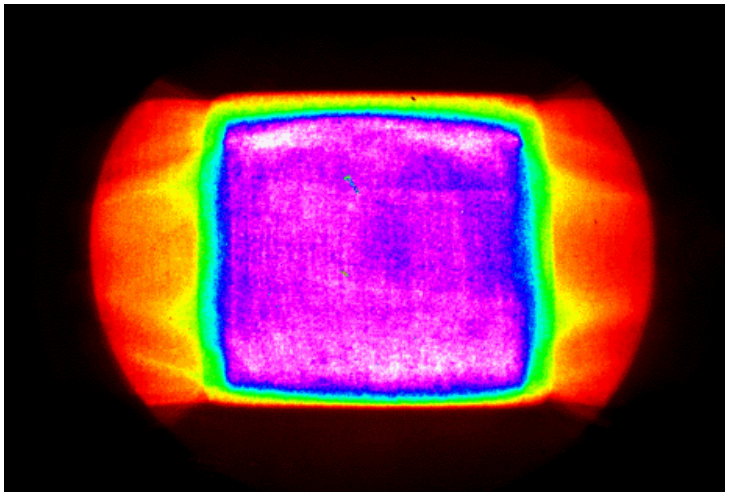

Figure 2. Measured intensity profile of diode laser source at the target plane.

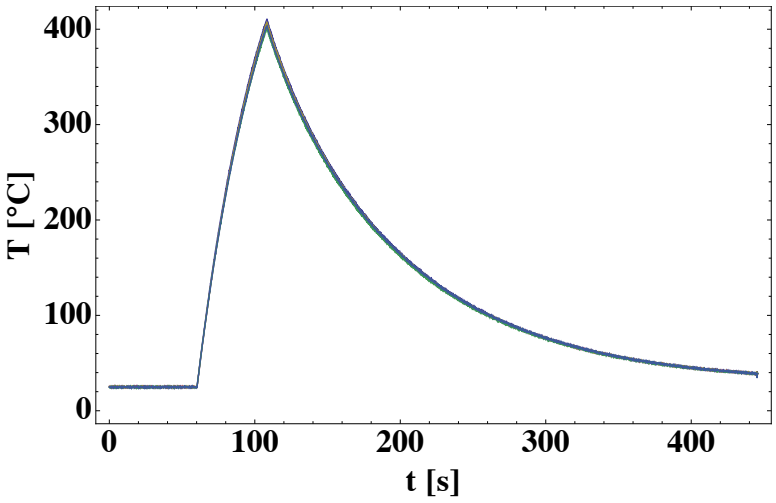

Figure 3. Temperature data recorded from five different thermocouples on a typical fresh aluminum sample. The measured temperatures from the different thermocouples are nearly identical and any difference is not visible on this scale.

The functions Q(T) and A(T) are calculated from the time derivative of the measured sample temperature, which is difficult to do accurately when the data is noisy. To improve numerical accuracy, data smoothing techniques described in the Appendix were used.

Measurements were made over a sufficiently broad range of sample temperatures; hence it was necessary to account for the temperature dependence of density and heat capacity of the metal sample. Data from [5], shown graphically in Figure 4, were used.

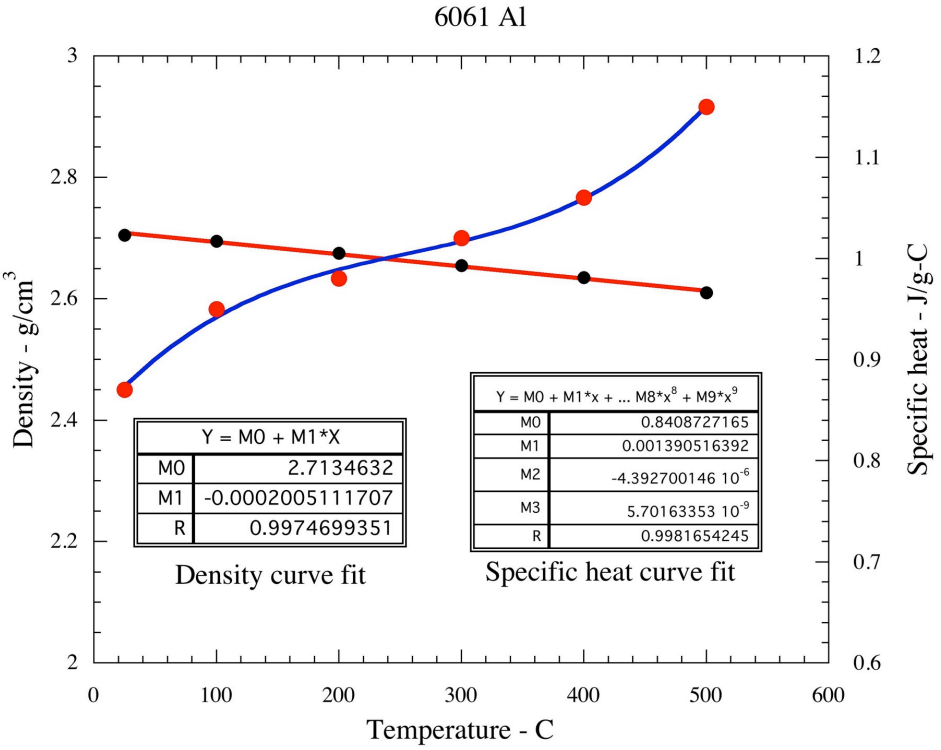

Figure 4. Density (red) and specific heat (blue) for aluminum 6061.

The resulting thermal loss curves, Q(T), calculated for several Al targets heated with laser intensity of 10 W/cm^2 and 20 W/cm^2 in various heating experiments are given in Figure 5, which shows that the thermal loss is a function only of the temperature, independent of heating rate.

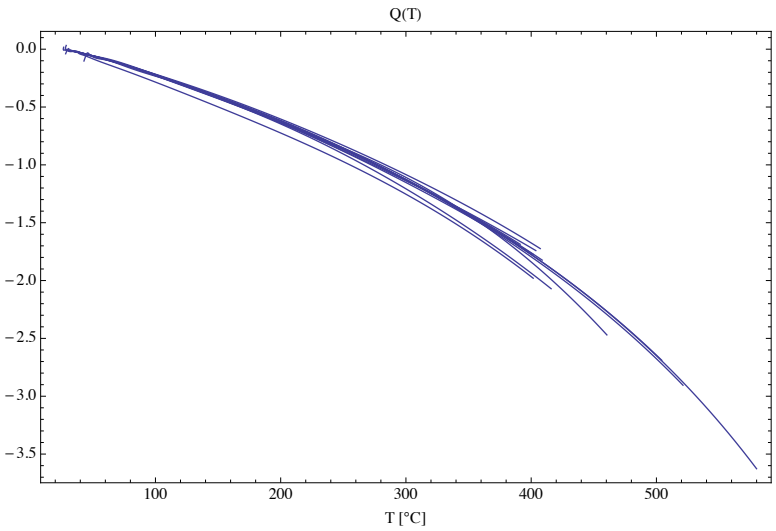

Figure 5. Q(T) calculated from a multiple data runs on aluminum at two different intensities.

Aluminum

Measurement

Comparison of absorption of Al before and after correction for thermal loss, shown in Figure 6, illustrates the importance of accounting for thermal losses. The loss-corrected results are found to be only weakly dependent on heating rate, justifying our approach. The absorptivity for Al is about 35% and nearly constant over this temperature range. Heating to 500°C did not produce any significant change in sample appearance or morphology, and repetitive measurements produced similar results.

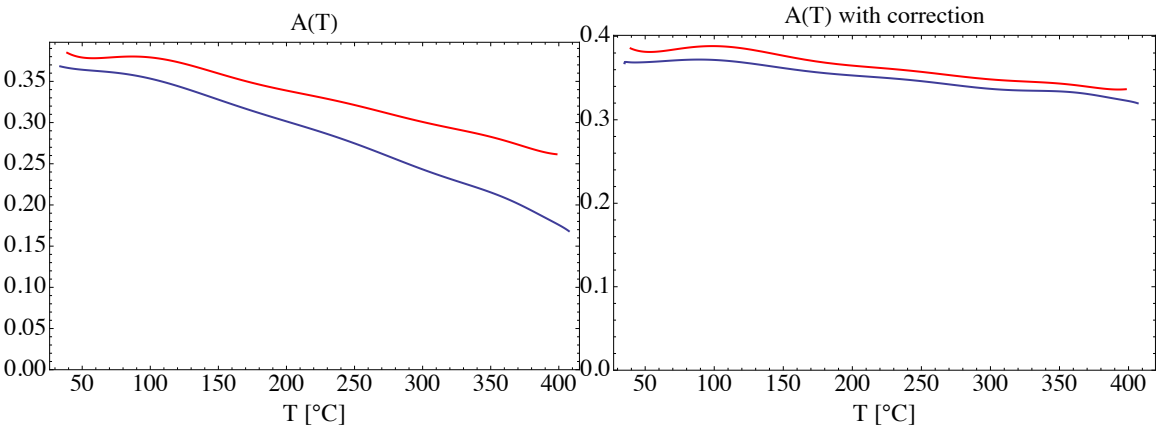

Figure 6. Absorption data before (left) and after (right) removal of thermal losses. The red curves correspond to absorptivity measured under 12 W/cm² intensity and blue curves under 24 W/cm². Small difference can be attributed to the sample differences or the accuracy of data processing.

Discussion

Absorption data for Al presented in textbooks [1] are measured for ideal, vacuum deposited films. Measurements here on as received, engineering grade, plate aluminum samples show much higher absorption, which is usually attributed to surface roughness, the presence of oxide films, and absorbing impurities [2]. The comparative magnitude of these effects and their wavelength dependence are discussed below.

Aluminum is one of the so-called near-free-electron (NFE) metals, for which electrons in the metal can be treated as a free-electron gas, with the addition of interband transitions [2]. The Drude model provides a good description of the dielectric constant. Figure 7 shows pure Al absorption as a function of wavelength for irradiation at normal incidence based on experimental measurements of the refractive index.

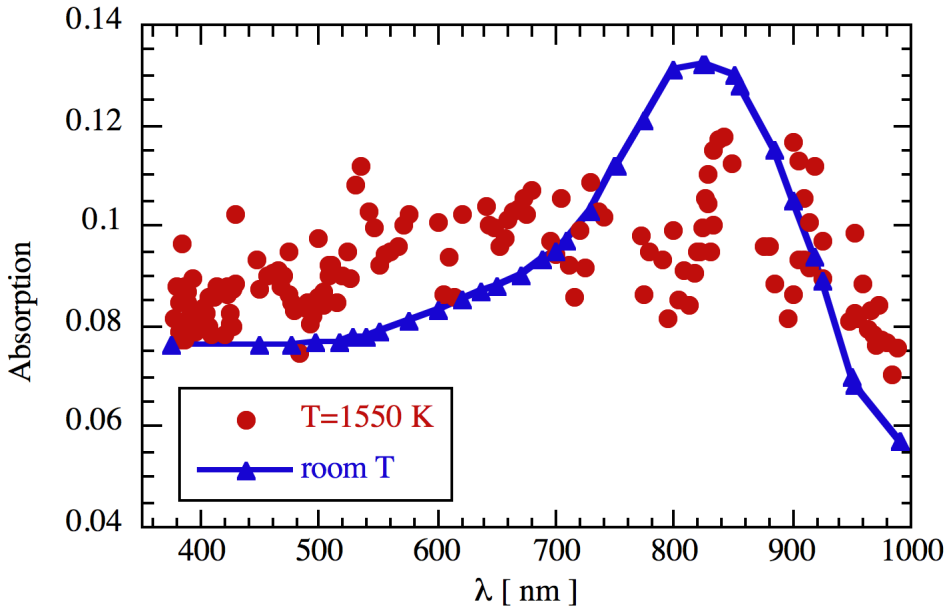

Figure 7. Experimental data of absorption versus wavelength for light incident normally on aluminum at room temperature (blue line [1]) and at 1550 K (red circles [6,7]).

Absorption typically increases with temperature, except for the resonance region, simply because the free electrons gain kinetic energy while the phonon population grows, which increases the electron-phonon collision frequency. Aluminum has an absorption peak at 820 nm due to an interband transition, which is shown clearly by the blue line in Figure 7. Absorption at 800 nm ($n = 2.767 + 8.48i$ for wavelength 0.795 μm) is about 13%, and 2.5 times higher than the absorption at 1 μm ($n = 1.27 + 10.41i$), while for 1.3-μm light ($n = 1.23 + 13.46i$) absorption falls to 2.3%. Absorption data for liquid Al (red dots in Figure 7) shows that elimination of the metal structure makes absorptivity wavelength independent.

Experimental data presented for 1-μm radiation absorption of bulk Al [2] demonstrates very different results, with absorption more than 4 times higher than measured for the ideal sample [1]. Also, the absorption is nearly temperature independent.

In real situations, aluminum is coated with an oxide layer that is transparent up to the UV range but has a high refractive index, $n = 1.62$ for wavelength 0.78 μm [2], that can change the reflectivity. The complex amplitude r of a wave reflected from the oxide film of thickness h on the aluminum substrate is given by [6]

$$r = \frac{r_{12}e^{-2i\varphi} + r_{23}}{e^{-2i\varphi} + r_{12}r_{23}}, \quad \varphi = \frac{\omega h}{c}\sqrt{n^2 - \sin^2\theta} \tag{2}$$

Here n is the oxide refractive index and $n_3 = 2.767 + 8.48i$ the complex refractive index of Al. r_{12} is the amplitude of the wave reflected from the bulk aluminum oxide, given by $r_{12} = (1-n)/(1+n) = -0.24$, r_{13} is the complex reflected amplitude from the bulk aluminum material. θ is the angle of incidence for the s-polarized wave. For the p-polarized, wave all data are related to the magnetic field amplitude. The complex value r_{13} is $r_{13} = (1-n_3)/(1+n_3) = -0.91 - 0.20i$. Reflectivity

from bulk Al at this wavelength is $R = \left|r_{13}\right|^2 = 0.87$ and absorptivity $A = 1 - R = 0.13$.

The value for r_{23} is given by $r_{23} = \dfrac{r_{12} - r_{13}}{r_{12} r_{13} - 1} = -0.84 - 0.30i$.

In the case of normal incidence, the calculated absorptivity as a function of the oxide layer thickness is presented in Figure 8, which shows that presence of the oxide layer can substantially increase absorption. For typical thickness of about 50 nm, absorption will be above 20%. Variability of the thickness will result in some average absorption value, but higher than predicted for pure aluminum. The reduction in absorptivity for a thicker oxide film, shown in Figure 8, results from wave interference in the film.

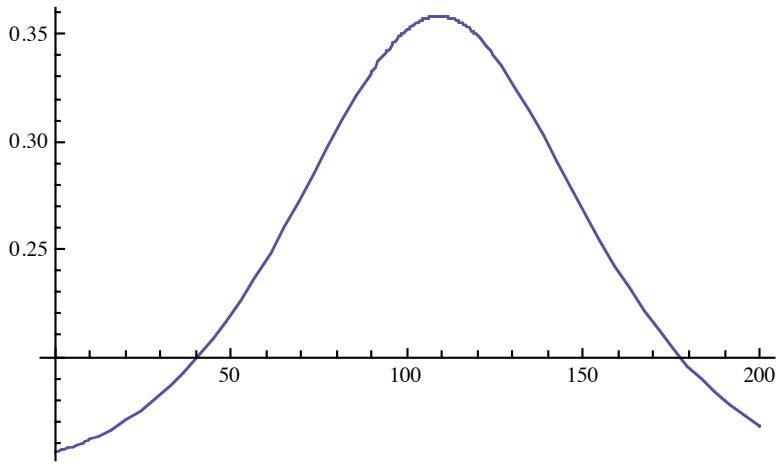

Figure 8. Absorptivity of Al coated by oxide film vs. film thickness in nanometers.

Thus, presence of an oxide film increases the absorptivity but not sufficiently to explain the observed results. The effect of the oxide layer is more noticeable for shorter wavelength light. The additional absorption is explained by surface roughness resulting in enhanced absorption and conversion of incident radiation to surface electromagnetic waves (plasmons). General calculations of absorption on a rough metal surface can be found, *e.g.* in [2], but are not helpful because usually detailed information about surface structure is not available.

The cold-rolled samples used for these measurements have parallel groves in the roll direction. Figure 9 shows absorption measured with the electric field of the

light parallel or orthogonal to the grooves. The higher absorption observed for the orthogonal field orientation is due to the fact that it is p-polarized with respect to the corrugated surface thus having higher absorption than the parallel field, which is s-polarized. These data directly demonstrate the effect of surface corrugations.

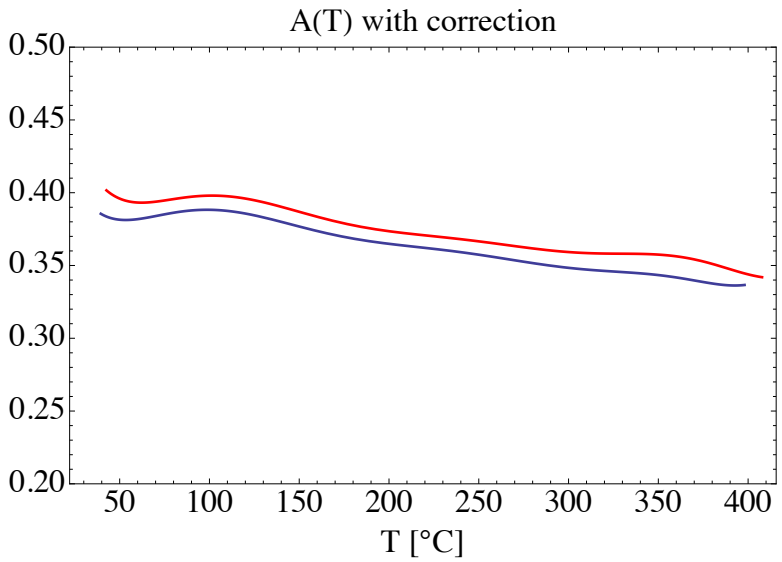

Figure 9. Absorptivity measurements with light polarized parallel (blue) and orthogonal (red) to the grooves direction. The intensity in both cases was

Heating the samples to 400°C does not cause irreversible material changes in Al, as repetitive measurements on the same sample gave the same results and there were no visible changes in the surface. However, when heated close to the melting temperature, ~580°C, some surface modification did occur as well as a noticeable increase in absorptivity when the sample was measured after cooling (see Figure 10). A possible source for this increase is modification of the oxide layer. Figure 8 showed that increasing the oxide layer thickness from 50 to 70 nm is sufficient to explain the results. Modification of surface roughness also may play a role.

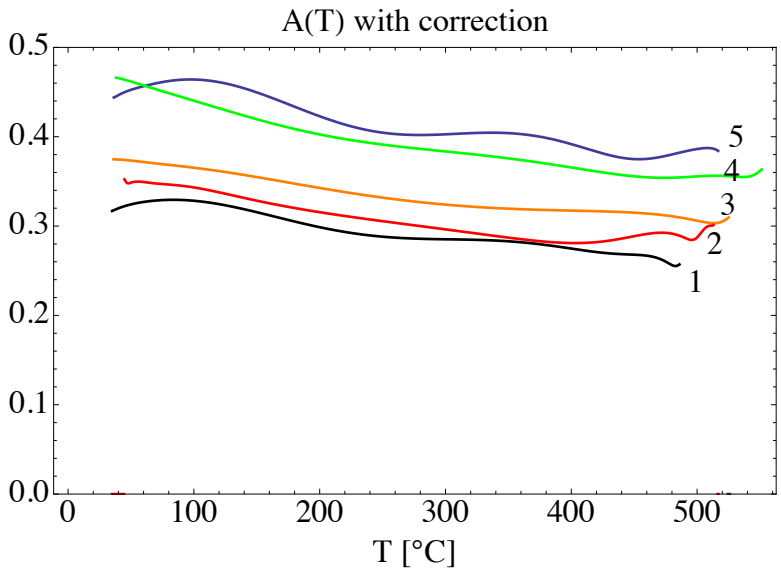

Figure 10. Al sample absorptivity in several heating and cooling cycles up to ~550°C. The increase in absorptivity is evidence for the modification of the oxide layer in Al.

Absorptivity measurements for Ti and steel samples

The experiments with Ti samples did not produce any additional complications (?). The temperature distribution over the sample was uniform, and readings of all thermocouples were the same. Experimental data were reproducible, and repetitive measurements gave the same results. Uniform changes in the metal color caused by irradiation were noticed, but these did not affect measured absorptivity of approximately 0.5 and only weakly dependent on temperature as shown in Figure 11.

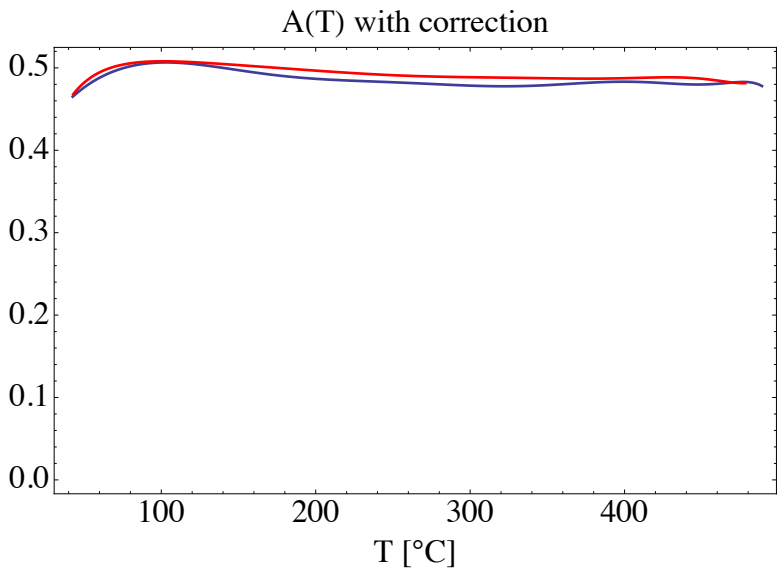

Figure 11. Measured Ti absorptivity in two consecutive heating and cooling experiments. The high repeatability suggest that no significant surface modification occur under the test conditions.

Absorptivity measured for 4030 steel on as-received samples was about 0.5 independent of temperature up to T~300° C, and generally increasing, but not uniformly, above this temperature. After the initial test, discolored spots could be seen on the sample surface, attributed to oxidation (see Figure 12). After cooling to room temperature, absorption measured on the already oxidized surface was about 0.8, higher than the as-received sample up to about 400C and then approximately the same at higher temperature. Temperature variations over the sample's surface resulting from changes in absorptivity at various locations on the surface due to the oxidation were observed. (see Figure 13). As a result, absorptivity is calculated using average temperatures measured by the thermocouples.

The importance of oxidation and its non-uniformity makes the absorptivity sensitive to the environment. For example, airflow, which affects oxidation [2,9], can increase absorptivity. The oxidation process also releases additional energy, which in our experiments can be counted as enhanced absorptivity.

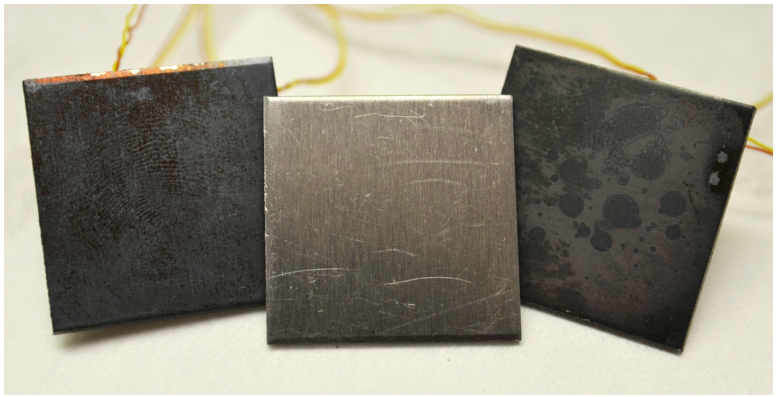

Figure 12. Steel oxides and changes color after irradiation. Seen at center is a fresh sample of steel 4030. The sample on the right was heated by direct laser illumination to ~800° C and discolored spots are clearly observed on the surface. The sample on the left had been used in several such tests the previous day now shows signs of rust on the surface.

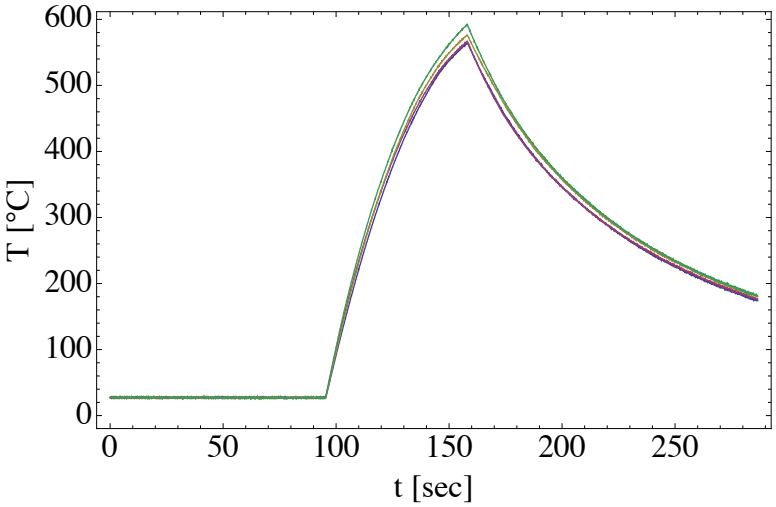

Figure 13. Thermocouples readings on a steel 4030 sample in a heating and cooling experiment. The difference in thermocouple readings is due to uneven surface oxidation.

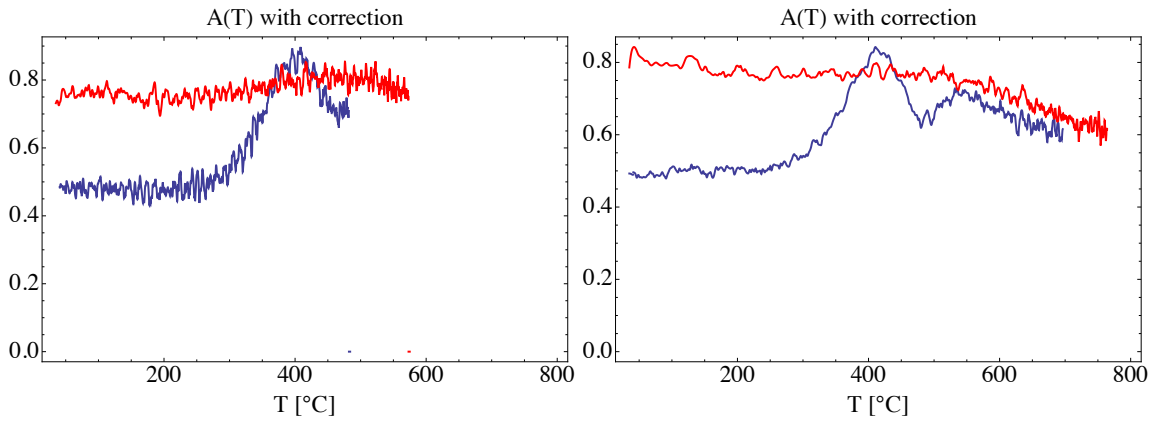

Figure 14. Data for two different steel samples under illumination of 12 W/cm² (left) and 24 W/cm² (right). The blue curve corresponds to the first illumination and red for the same sample under second illumination at the same intensity.

Thermal losses

Thermal loss consists of two primary components: convective cooling and thermal radiation. At low temperatures, radiative loss is small and can be disregarded. The heated surface induces convective flow near it, which cools the sample. Convective flow near a vertical wall is characterized by the Grashof number Gr,

$$Gr = \frac{\beta g x^3 \Delta T}{\nu^2} = \frac{g x^3 \Delta T}{\nu^2 T}, \quad \beta = -\frac{\partial \rho}{\rho \partial T} \approx \frac{1}{T} \tag{3}$$

Here g is the gravitational acceleration, ν the air kinematic viscosity, x the sample size, ΔT the difference between the sample temperature T and ambient temperature. For developed convection, $Gr \gg 1$. In our case, for $x = 3$ cm, $\Delta T = 100$, T = 400 K, $Gr \sim 10^5 \gg 1$.

The cooling flux is given by the expression

$$P_T = \frac{\kappa}{x} Nu \Delta T \tag{4}$$

where κ is the air heat conduction and Nu the Nusselt number. For our range of Gr, $Nu \sim \frac{1}{2} Gr^{1/4}$ [9]. Account must be taken that viscosity and thermal conduction vary with temperature:

$$\nu = \nu_0 \left(T / T_0\right)^{3/2}, \quad \kappa = \kappa_0 \left(T / T_0\right)^{1/2} \tag{5}$$

The above value of the Nusselt number was obtained for experiments with temperature independent viscosity and thermal conduction. We fitted our data with the same expression (4) with viscosity and thermal conduction taken at sample temperature and an adjustable numerical coefficient c. Thus the thermal flux can be represented as

$$P_T = 2c \cdot 0.85 \kappa_0 \Delta T \left(\frac{g}{x\nu_0}\right)^{1/4} \left(\frac{T_0 \Delta T}{T^2}\right)^{1/4} \tag{6}$$

Here, the factor 2 accounts for convection losses from each side of the sample. At room temperature, $\kappa_0 = 2 \times 10^{-4} \dfrac{W}{cm \cdot K}$ and $\nu_0 = 0.157 \text{ cm}^2 / s$. For $x = 3$ cm,

$$P_T = 2c \cdot 1.2 \times 10^{-3} \Delta T \left(\frac{T_0 \Delta T}{T^2}\right)^{1/4} \frac{W}{cm^2 K} \tag{7}$$

It was found that c~1.7 agreed well with our experimental data.

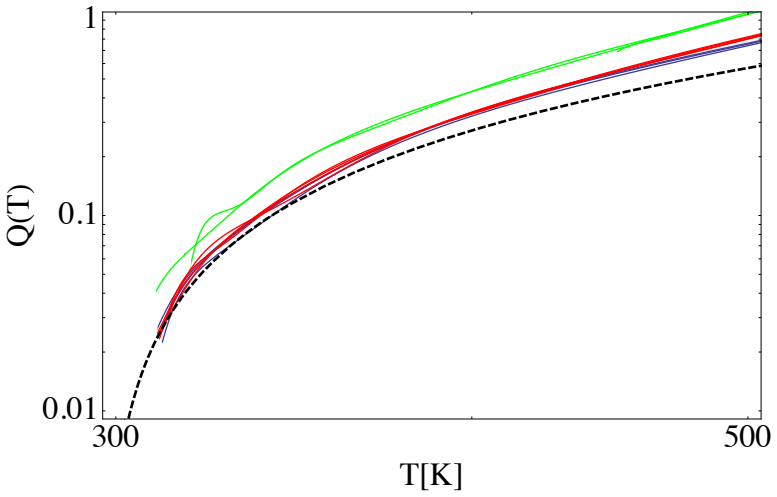

Figure 15. Measured thermal losses Q(T) for several experimental tests on Al (red), Ti (blue) and steel 4030 (green) samples. Dashed line represents an estimate for convective cooling in accordance with Eq. (7).

Comparison of Eq. (6) with $c = 1.7$ and experimental data for Al, Ti and steel samples is presented on Figure 15. At low temperatures, Eq. (7) provides a good description of convective losses and the losses for Al and Ti are similar. The convection losses are independent of materials. At higher temperature, losses exceed those given by the Eq. (7) due to radiative losses and will be discussed later.

The above estimates were made for steady state convection. It can be different in non-stationary regime. Let us estimate the time for steady state flow onset. Heat diffuses from the sample surface to the air over the distance $\delta \sim \sqrt{Dt}$, inducing convective flow with velocity u. In convective flow, buoyancy is compensated by viscosity

$$\frac{\nu u}{\delta^2} \sim g\beta\Delta T, u \sim \frac{g\beta\Delta T D t}{\nu} \tag{8}$$

In steady state, the vertical temperature convection is compensated by lateral thermal transport

$$\frac{u\Delta T}{x} \sim \frac{D\Delta T}{\delta^2} \tag{9}$$

Combining the last two equations one gets for the onset time:

$$t \sim \sqrt{\frac{\mathrm{Pr}\, x}{g\beta\Delta T}} = \sqrt{\frac{\mathrm{Pr}\, xT}{g\Delta T}} \tag{10}$$

For T~300°C, $x = 3$ cm, and Pr~0.7 in air, the onset time is small, $t \approx 0.06$ seconds. Practically, the convection is expected to be in stationary regime. This conclusion is consistent with the absorptivity results that were measured for different pump intensities.

Now, with an estimate for the convective loss, one can subtract it from Q(T) and obtain the radiative losses. The convective losses are independent of material but sensitive to the sample geometry. Radiative losses are independent of geometry but sensitive to the material. Data for Al and Ti will be presented.

The intensity of thermal radiation according to Kirchhoff law can be related to the blackbody radiation $I_{bb}(\lambda)$ and reflectivity R_λ [9]:

$$I_\lambda = \varepsilon_\lambda I_{bb}(\lambda) = (1 - R_\lambda) I_{bb}(\lambda) \tag{10}$$

Total emissivity is obtained after averaging over all angles and wavelengths

$$\varepsilon = \frac{\int I_\lambda \, d\lambda \, d\Omega}{\int I_{bb}(\lambda) d\lambda \, d\Omega} = \frac{\int I_\lambda \, d\lambda \, d\Omega}{\sigma T^4} \tag{11}$$

The emissivity is related to the absorptivity and sensitive to the surface quality and change from sample to sample. As a result, there is considerable variability in emissivity data [9]. In our specific case the emissivity is given by

$$\varepsilon = \frac{Q(T) - P_T}{\sigma T^4 - \sigma T_0^{\,4}} \tag{12}$$

The graph of emissivity for Al and Ti calculated from Eq. (12) presented on Figure 16.

The data are averaged over few samples. Let us mentioned the variability from sample to sample is not small – larger than 20%. Nevertheless the data are consistent with Figure 15: steel radiates more the Ti and Ti more then Al.

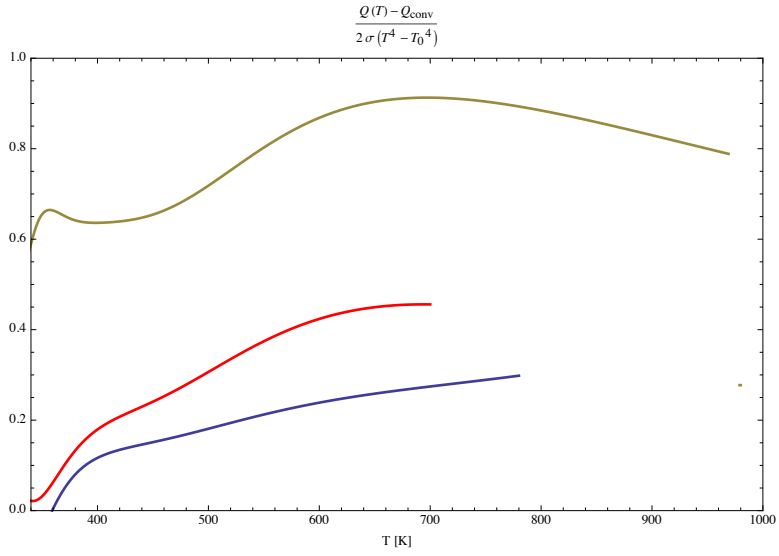

Figure 16. Emissivity calculated from Eq. (12) for several metals: Al 6161 (blue), Ti (red), steel 4130 (brown).

Conclusion

To the best of our knowledge, the first measurements of absorptivity of 0.8 μm light by industrial grade metals over a broad temperature range are presented. The measurements were performed utilizing a calorimetric set-up. The use of laser diodes as a light source makes possible the uniform irradiation of large samples increasing measurement accuracy. It was shown that thermal losses due to convection and thermal radiation play an important role in energy balance and must be taken into account. A method to subtract thermal losses to derive absorptivity at elevated temperatures was demonstrated. It was found that up to the temperature of ~500°C the absorptivity of Al weakly varies with temperature, consistent with measurements at 1.3 μm [3] and almost two times higher then absorptivity at 1 μm [2]. This result is expected due to the interband transition peak near 825 nm. The absorptivity of Ti is also insensitive to the temperature and comparable with absorptivity at 1 μm. Measurements on steel showed that oxidation can affect absorptivity. As oxidation occurs non-uniformly over the sample, the local absorptivity also varies and one can only talk about average absorptivity values. Evaluation of the thermal losses, which may be derived from our measurements, also provides useful information about convective and radiative losses. Finally, methods presented here can be applied in measurements of absorptivity for a variety of materials using laser diodes or other laser sources with different wavelengths.

Appendix

Differentiation of noisy experimental data is typically unreliable, so we describe two smoothing techniques: least-squares polynomial fit and Savitzky-Golay derivative filter. Since the temperature signal is a well-behaved monotonic function during heating and cooling, finding least-squares polynomial fits for the recorded data over the heating and cooling periods is simple and produces fairly good approximations. We found 10^{th}-order polynomial fits to the measured data followed by differentiation in some of our thermal calculations. In other cases, we utilized the method of least squares described by Savitzky and Golay [4], where a given number of data points are fitted to a low-order polynomial via a least-squares procedure to obtain the value of the smoothing interpolant at the center of the interval. The least-squares calculations may be carried out by convolution of the data points with properly chosen sets of integers. This method assumes that the data is evenly spaced and without breaks. Due to technical issues, our recorded time series data usually contain uneven spacing and short breaks where no useful data is recorded. This poses no problems for the polynomial fit algorithm but offers some complications when one tries to apply Savitzky-Golay filters directly. Because in almost all cases, the simplistic polynomial fit agrees very well with the approximation found via the more sophisticated Savitzky-Golay method, as seen in Figure 17, both of these methods were applied interchangeably and without distinction.

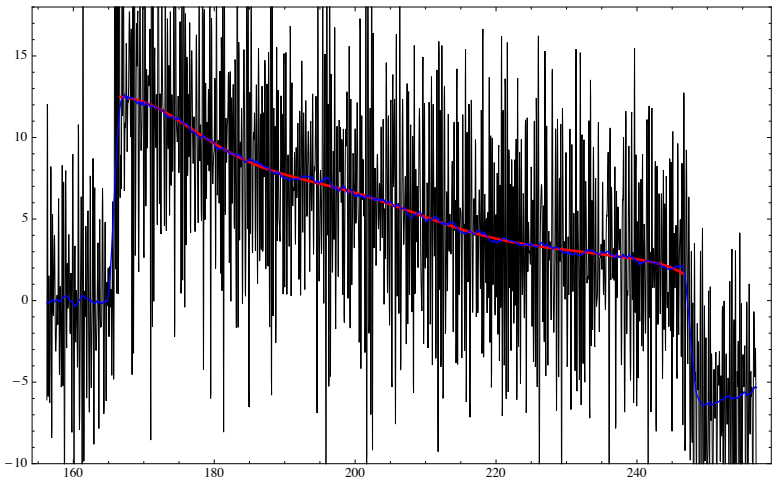

Figure 17: Comparison of traces produced by direct differentiation of measured data (grey), 21 point quadratic Savitzky-Golay derivative filter (blue), 10th order polynomial fit of measured data followed by differentiation (red).

References

1. Handbook of optical constants of solids, ed. E.D. Palik, Academic Press, San Diego, CA (1998).

2. A.M. Prokhorov , V.I. Konov ,I. Ursu , I.N. Mihailescu, Laser Heating of Metals. Adam Higler Bristol (1990).

3. R.K. Freeman, F.A. Rigby, N. Morley, “Temperature-Dependent Reflectance of Plated Metals and Composite Materials Under Laser Irradiation”, J. Thermophysics and Heat Transfer, 14(3), 305-312 (2000).

4. A. Savitzky, M. Golay, “Smoothing and Differentiation of Data by Simplified Least Squares Procedures”, Anal. Chem., 36(8), 1627-1639 (1964).

5. K.G. Mills, Recommended Values of Thermophysical Properties for Selected Commercial Alloys, Woodhead Publishing, Cambridge, England (2002).

6. S. Krishnan, P.C. Nordine, "Optical Properties of Liquid Aluminum in the Energy Range 1.2-3.5eV", Phys. Rev. B, 47(18), 11780(1993).

7. S. Krishnan and P.C. Nordine, "Analysis of the optical properties of liquid aluminum", Phys. Rev. B, 48(6), 4130(1993).

8. L. Landau, E. Lifshitz Electrodynamics of Continuous Media, Pergamon Press (1960).

9. E.Eckert, R.Drake Analysis of heat and mass transfer McGraw Hill 1972